Single-Frame Super-Resolution via Compressive Sampling on Hybrid Reconstructions

Ji-Ping Zhang(✉), Tao Dai, and Shu-Tao Xia

Graduate School at Shenzhen, Tsinghua University,
Shenzhen 518055, Guangdong, China
{zjp13,dait14}@mails.tsinghua.edu.cn, xiast@sz.tsinghua.edu.cn

Abstract. It is well known that super-resolution (SR) is a difficult problem, especially the single-frame super-resolution (SFSR). In this paper, we propose a novel SFSR method, called compressive sampling on hybrid reconstructions (CSHR), with high reconstruction quality and relatively low computation cost. It mainly depends on the combination of the results of other SR methods, which are characteristic of high speed and low quality SR results alone. As a result, CSHR inherits the merit of low computation cost. We resample those low quality SR results in DCT domain instead of in pixel domain and regard the similar expansion coefficients as consensus which would be compressively sampled later. In CSHR, obtaining a high resolution image is only to solve a convex optimization program. We use compressed sensing theory to ensure the efficiency of our method. Also, we give some theoretic results. Experimental results show the effectiveness of the proposed method when compared to some state-of-the-art methods.

Keywords: Image processing · Single-frame super-resolution · Compressed sensing · Signal processing

1 Introduction

Image super-resolution (SR) is to recover a high resolution (HR) image from a series of low resolution (LR) images. SR is one of the most spotlighted research as it can overcome the limitation of hardware, such as the chip size, shot noise and diffraction in digital imaging system. Depending on the number of LR images, the recovery methods could be divided into two categories: single-frame super-resolution (SFSR) and multi-frame super-resolution (MFSR). Our research mainly focus on the SFSR problem.

The basic method for approximating a solution to SR recovery is through conventional linear interpolators, of which the bicubic interpolator is highly preferable. These SR methods and their variants have been elaborated by Park et al. [8] and Van [11]. Besides classical interpolation methods, another representative SR method is based on sparse representation of low and high resolution (LHR) patch-pairs over a dictionary pair. Yang et al. [13,14] propose a method working

S. Arik et al. (Eds.): ICONIP 2015, Part III, LNCS 9491, pp. 610–618, 2015.
DOI: 10.1007/978-3-319-26555-1_69

directly with the LR training patches and their features, which does not require any learning on the HR patches. The LR image is viewed as a downsampling version of the HR image, whose patches are assumed to have a sparse representation with respect to an over-complete dictionary of prototype signalatoms. Zeyde et al. [15] embark from Yang et al., and assume a local Sparse-Land model on image patches served as regularization.

The most important advantage of the interpolation based methods is that it contains low computation cost. However, the reconstruction quality is much poorer than sparse representation based methods, because the degradation models are limited: they are only applicable when the blur and the noise characteristics are the same for all LR images. Conversely, sparse representation of LHR patch-pairs over a dictionary has a better reconstruction quality with higher computational complexity. In practice, SFSR is an ill-posed problem due to the insufficient number of observations and the unknown registration parameters. No one knows what the original HR image exactly is. Fortunately, the only thing we can be sure of is that all of the SR reconstructions must be similar to each other, though different SR reconstructions are not exactly same to each other. Since the problem is that we have several SR reconstructions for the same HR image, yet how to use them to get a better reconstruction?

In this paper, we propose a novel compressive sampling on hybrid reconstruction (CSHR) method with a high reconstruction quality and low computation cost. It is mainly based on some low computation cost and low reconstruction quality methods' results. In order to focus on our method, we mostly deal with SFSR, although our method can be readily extended to handle multi-frame super-resolution. In CSHR, we are focusing on the common view (the same part) of different SR results. Even though there may be less consensus, compressed sensing (CS) [2,4] asserts that we can recover certain signals from many fewer samples or measurements than the traditional methods. Thus we could use CS to recover the HR by the limited consensus. CS is good at signal processing, however, it does not work well in image processing directly. Therefore, we transform other different SR results into an appropriate basis, which can be efficiently solved by CS. And we regard the similar expansion coefficients as consensus in that appropriate basis. Then we do compressive sampling on these consensus. Finally, we recover the HR image by solving a convex optimization program. Besides, we have proved that with a high probability, the coherence between sensing basis Φ and representation basis Ψ in CSHR is less than $\sqrt{2 \log N}$. Therefore, CS theory ensures the probability of CSHR's success. Unlike the aforementioned sparse representation of LHR, our method does not rely on any learning patches or over-complete dictionary. Consequently, CSHR works more efficiently.

The rest of this paper is organized as follows. Section 2 presents our CSHR method. We evaluate the performance of our CSHR method in Sect. 3 both in visual appearance and numerical criteria, and compare it with state-of-the-art methods for SFSR. Section 4 concludes the whole paper.

2 Compressive Sampling on Hybrid Reconstructions

2.1 Observation Model

Our observation model is based on Park's [8] multi-frame observation model. Supposing the resolution of the original HR image $\boldsymbol{x}$ is $L_1N_1 \times L_2N_2$, we rewrite it in the form of a vector $\boldsymbol{x} = [x_1, x_2, \ldots, x_N]^T$, where $N = L_1N_1 \times L_2N_2$. After downsampling the HR image $\boldsymbol{x}$ with horizontal scale factor L_1 and vertical scale factor L_2, we get the LR image $\boldsymbol{f}$ of which the resolution is $N_1 \times N_2$. Similarly, we rewrite it in the form of a vector $\boldsymbol{f} = [f_1, f_2, \ldots, f_M]^T$, where $M = N_1 \times N_2$. Now, the image acquisition process could be expressed as follows:

$$\boldsymbol{f} = W\boldsymbol{x} + \boldsymbol{n} \tag{1}$$

where W is a $M \times N$ sampling matrix which denotes the warping, blurring and downsampling during the image acquisition and $\boldsymbol{n}$ is a $M \times 1$ vector which denotes the additive noise. There are two main differences between our model and Park's:

1. We convert the Park's MFSR model to our SFSR model.
2. We do not consider the sub-pixel movement in matrix W as Park did, for we focus on the SFSR problem. Hence, image registration is useless in our method.

2.2 Compressive Sampling on Consensus

Supposing we have known K different SR methods whose results are corresponding to: $\tilde{\boldsymbol{x}}_1, \tilde{\boldsymbol{x}}_2, \ldots, \tilde{\boldsymbol{x}}_K$. We regard $\tilde{\boldsymbol{x}}_k$ as one of K different estimations for the HR $\boldsymbol{x}$. Before we go further, let us take a look at the estimation $\tilde{\boldsymbol{x}}_k$. Equation (1) tells us that the SFSR is an ill-posed problem: what we only have is an LR observation $\boldsymbol{f}$. By estimating the sampling matrix W and modeling the noise $\boldsymbol{n}$, we are able to find the HR image $\tilde{\boldsymbol{x}}_k$ which satisfies (1). No one knows what the HR image $\boldsymbol{x}$ exactly is, however, the only thing we can be sure of is that all the $\tilde{\boldsymbol{x}}_k$ must be similar to $\boldsymbol{x}$, otherwise the kth SR method is not a good recovery method. Though different estimations are not exactly same to each other, they must be similar to each other because of the transitive relation. In this paper, we focus on the common part of different $\tilde{\boldsymbol{x}}_k$. We will transform the $\tilde{\boldsymbol{x}}_k$ into an appropriate basis and then use the similar expansion coefficients.

At the beginning, we transform the estimation $\tilde{\boldsymbol{x}}_k$ into a different domain Ψ instead of in pixel domain:

$$\tilde{\boldsymbol{y}}_k = \Psi\tilde{\boldsymbol{x}}_k \tag{2}$$

The basis Ψ has the size of $m \times N$ in (2). Ideally, $\tilde{\boldsymbol{x}}_k$ has a sparse representation on the basis Ψ. The main role of the basis Ψ is to let the l_0-norm of the binary support vector $\|\boldsymbol{s}_y\|_{l_0}$ in (3) as large as possible, that is non-zero elements in $\boldsymbol{s}_y$ as much as possible. It gives us representation of continuous image projected onto discrete domain. Different choices of Ψ allow us to choose the domain in which we decide to sample the image.

Then we look for a $m \times 1$ binary vector $\boldsymbol{s}_y$ as a support for all $\tilde{\boldsymbol{y}}_k$:

$$\tilde{\boldsymbol{y}}' = \boldsymbol{s}_y \cdot \tilde{\boldsymbol{y}}_k \qquad (k = 1, 2, \ldots, K) \tag{3}$$

In (3) denotes element-by-element multiplication and $\tilde{\boldsymbol{y}}'$ is the consensus of all $\tilde{\boldsymbol{y}}_k$. Equation (3) means that we could abstract the consensus of all $\tilde{\boldsymbol{y}}_k$ to $\tilde{\boldsymbol{y}}'$ by the support $\boldsymbol{s}_y$. In other words, the support $\boldsymbol{s}_y$ is like a mask which retains all the similar expansion coefficients in K different $\tilde{\boldsymbol{y}}_k$.

Supposing Φ_y is a $p \times m$ binary random matrix. In compressive sensing, we could regard Φ_y as a sensing basis, however, it does not work efficiently since it senses too much noise which is not the consensus we need. In fact, we hope to sample the consensus $\tilde{\boldsymbol{y}}'$. Here, we could use a trick by the support vector $\boldsymbol{s}_y$: let $S_y = [\boldsymbol{s}_1, \boldsymbol{s}_2, \ldots, \boldsymbol{s}_p]^T$, where $\boldsymbol{s}_1 = \boldsymbol{s}_2 = \cdots = \boldsymbol{s}_p = \boldsymbol{s}_y$. Now we have got a $p \times m$ matrix Ψ which satisfies:

$$\Phi = \Phi_y \cdot S_y \tag{4}$$

If we use the Φ as a sensing basis:

$$\hat{\boldsymbol{y}} = \Phi \tilde{\boldsymbol{y}}_k \qquad (k = 1, 2, \ldots, K) \tag{5}$$

we could find that:

$$\hat{\boldsymbol{y}} = \Phi_y \tilde{\boldsymbol{y}}' \tag{6}$$

$\hat{\boldsymbol{y}}$ is the sampling result on the consensus which is what we need. Equation (5) means that we could sample the consensus of all $\tilde{\boldsymbol{y}}_k$ to $\hat{\boldsymbol{y}}$.

For example, let $K = 4$, $m = 4$, we have $\tilde{\boldsymbol{y}}_1 = \begin{bmatrix} 1 \\ 7 \\ 8 \\ 7 \end{bmatrix}$, $\tilde{\boldsymbol{y}}_2 = \begin{bmatrix} 1 \\ 8 \\ 7 \\ 7 \end{bmatrix}$, $\tilde{\boldsymbol{y}}_3 = \begin{bmatrix} 1 \\ 7 \\ 7 \\ 7 \end{bmatrix}$, $\tilde{\boldsymbol{y}}_4 = \begin{bmatrix} 1 \\ 8 \\ 8 \\ 7 \end{bmatrix}$, obviously, $\boldsymbol{s}_y = \begin{bmatrix} 1 \\ 0 \\ 0 \\ 1 \end{bmatrix}$, and the consensus $\tilde{\boldsymbol{y}}' = \begin{bmatrix} 1 \\ 0 \\ 0 \\ 7 \end{bmatrix}$. Supposing $p = 2$ and $\Phi_y = \begin{bmatrix} 1\,0\,1\,0 \\ 1\,1\,0\,1 \end{bmatrix}$, $S_y = \begin{bmatrix} 1\,0\,0\,1 \\ 1\,0\,0\,1 \end{bmatrix}$, then $\Phi = \begin{bmatrix} 1\,0\,0\,0 \\ 1\,0\,0\,1 \end{bmatrix}$, and we will get $\hat{\boldsymbol{y}} = \begin{bmatrix} 1 \\ 8 \end{bmatrix}$.

Meanwhile, we will look for another $N \times 1$ support $\boldsymbol{s}_x$ which satisfies:

$$\tilde{\boldsymbol{x}}' = \boldsymbol{s}_x \cdot \tilde{\boldsymbol{x}}_k \qquad (k = 1, 2, \ldots, K) \tag{7}$$

a binary random matrix Θ_x, the size of which is $r \times N$, let $S_x = [\boldsymbol{s}_1, \boldsymbol{s}_2, \ldots, \boldsymbol{s}_r]^T$, where $\boldsymbol{s}_1 = \boldsymbol{s}_2 = \cdots = \boldsymbol{s}_r = \boldsymbol{s}_x$, and then we will get

$$\Theta = \Theta_x \cdot S_x \tag{8}$$

Θ in (8) satisfies:

$$\hat{\boldsymbol{x}} = \Theta \tilde{\boldsymbol{x}}_k \qquad (k = 1, 2, \ldots, K) \tag{9}$$

Equation (9) is similar to (5): $\hat{\boldsymbol{x}}$ is the similar coefficients hybrid mixture abstracted from the K different $\tilde{\boldsymbol{x}}_k$ by the $r \times N$ matrix Θ.

Finally, our problem is converted to recover a vector $\boldsymbol{x}$ from equation:

$$\hat{\boldsymbol{y}} = A\boldsymbol{x} \tag{10}$$

where $A = \Phi\Psi$ is a $p \times N$ new sampling matrix telling us information about $\boldsymbol{x}$ on basis Ψ. Moreover, the solution $\boldsymbol{x}$ in (10) should obey (9), which means our result must be agree with the consensus of all $\tilde{\boldsymbol{x}}_k$.

2.3 Recovery

CS recovery uses nonlinear approximation in the transform domain, although the measurements in (10) is linear. To solve (10) the recovery can be simplified to solving the following convex program:

$$\min_{\hat{\boldsymbol{x}}} \|\Omega\hat{\boldsymbol{x}}\|_{l_1} \qquad \text{subject to} \qquad A\hat{\boldsymbol{x}} = \hat{\boldsymbol{y}} \tag{11}$$

Equation (11) means that we find a N-dimention vector $\hat{\boldsymbol{x}}$ which is the sparsest in the transform domain Ω that satisfies the measurements we observed. The constraint $A\hat{\boldsymbol{x}} = \hat{\boldsymbol{y}}$ means that we only consider the results which could produce the same measurements $\hat{\boldsymbol{y}}$ which we have observed. The l_1 norm is the sum of magnitude:

$$\|\boldsymbol{z}\|_{l_1} = \sum_{i=1}^{n} |z_i| \tag{12}$$

where $\boldsymbol{z} = \Omega\hat{\boldsymbol{x}}$. The reasons of using l_1 norm are: (i) sparse signal have small l_1 norm relative to its energy, (ii) it is convex that makes the optimization solvable [10].

2.4 Stability

The main result of CS theory [3,5] is that the number of measurements we need to recover the image does depend on the complexity of image representation in the domain we choose rather than the number of pixels we wish to recover.

CS is mainly concerned with low coherence pairs. The coherence between Φ and Ψ is defined as follows:

$$\mu(\Phi, \Psi) = \sqrt{N} \cdot \max_{1 \le i,j \le N} |\langle \phi_i, \psi_j \rangle| \tag{13}$$

which means the largest correlation between any two elements of Φ and Ψ [6]. If Φ and Ψ contain correlated elements, the coherence $\mu(\Phi, \Psi)$ is large, otherwise, it is small.

From (4) we know that Φ is the result of $\Phi_y \cdot S_y$,

$$\mu(\Phi, \Psi) \le \min(\mu(\Phi_y, \Psi), \mu(S_y, \Psi)) \tag{14}$$

Since Φ_y is a binary random matrix, with a high probability, the coherence between Φ_y and Ψ is about $\sqrt{2\log N}$. Hence with a high probability, the coherence between Φ and Ψ is less than $\sqrt{2\log N}$, which indicates that Φ and Ψ are incoherent. A most important theorem in CS [1] is that if $\boldsymbol{x}$ in our transform domain Ψ is S-sparse, select p measurements in the Ψ domain uniformly at random. Then if

$$p \geq C \cdot \mu^2(\Phi, \Psi) \cdot S \cdot \log N \tag{15}$$

for some positive constant C, the solution to (11) is exact with overwhelming probability. It is shown that the probability of success exceeds $1 - \delta$ if $p \geq C \cdot \mu^2(\Phi, \Psi) \cdot S \cdot \log(N/\delta)$.

In a word, CS theory preserves that $\boldsymbol{x}$ can be exactly recovered from our CSHR by minimizing a convex function. Solving the convex program does not need to assume any knowledge about the number of nonzero coordinates of $\hat{\boldsymbol{y}}$, their locations, or their amplitudes which we assume all completely unknown priori.

3 Experimental Results

In this section, we simulated experiments to demonstrate the performance of our CSHR method by using several standard benchmark test images[1]. During the simulation scenario, we first downsample the HR test image $\boldsymbol{x}$ with both horizontal and vertical scale factor of 2 as the LR image $\boldsymbol{f}$. Then, we recover the image $\tilde{\boldsymbol{x}}_k$ by using Nearest neighbor, Bilinear, Bicubic, ScSR [14] and TIP14 [9]. Based on these $K = 5$ fundamental methods, we use DCT basis as Ψ and Ω. Figures 1 and 2 gives us a visual comparison on the partial of original images.

(a) Original image (b) ScSR[14] (c) TIP14[9] (d) **CSHR**

Fig. 1. Visual comparison on Babbon.

In addition to subjective visual comparison, we also provide the peak-signal-to-noise ratio (PSNR) [7] as well as the structural similarity index measure (SSIM) [12] in Table 1 which are used quantitatively to measure the results of different SR methods[2]. PSNR is a traditional criterion that is widely used in signal fidelity, while SSIM is known to be more consistent with human visual system (HVS). Results with larger PSNR and SSIM are considered to have better results.

[1] http://sipi.usc.edu/database/database.php?volume=misc.
[2] More results are shown in https://gist.github.com/Brilliant/7472969d4020599a13d0.

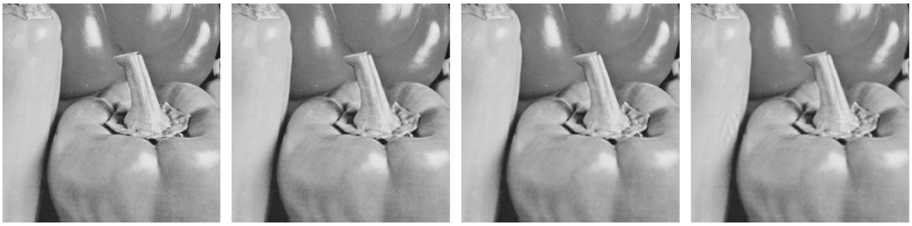

(a) Original image (b) ScSR[14] (c) TIP14[9] (d) **CSHR**

Fig. 2. Visual comparison on Peppers.

Table 1. Comparison based on PSNR (dB) and SSIM

Images	NN	Bilinear	Bicubic	ScSR	TIP14	CSHR
Airplane (U-2) 7.2.01	34.1285	34.0964	34.4150	34.7347	34.6681	**35.0588**
	0.8160	0.8031	0.8188	0.8383	0.8312	**0.8459**
Car and APCs 7.1.10	33.3599	33.9880	34.9014	35.8014	35.7503	**36.2948**
	0.8574	0.8605	0.8867	0.9106	0.9072	**0.9177**
Girl (Lena, or Lenna) 4.2.04	31.4187	32.6780	34.1092	36.1288	36.2255	**36.4926**
	0.8960	0.9028	0.9198	0.9367	0.9358	**0.9419**
Man 5.3.01	29.9675	30.8534	32.0520	33.8399	**33.8780**	33.8498
	0.8571	0.8599	0.8865	0.9133	0.9111	**0.9145**
Mandrill (a.k.a. Baboon) 4.2.03	23.1195	23.0403	23.6253	24.3864	24.3946	**24.8038**
	0.6979	0.6553	0.7116	0.7810	0.7775	**0.7882**
Peppers 4.2.07	29.7547	30.9894	31.7423	32.8905	32.7709	**33.2834**
	0.8624	0.8715	0.8843	0.8997	0.8973	**0.9019**
Tank 7.1.07	30.2140	30.4347	31.1732	31.9449	31.9254	**32.3743**
	0.7914	0.7793	0.8166	0.8544	0.8490	**0.8625**
Tank 7.1.09	30.0818	30.2545	30.9968	31.8264	31.7971	**32.3024**
	0.7921	0.7771	0.8150	0.8551	0.8493	**0.8636**
Truck and APCs 7.1.05	28.9856	29.3136	30.0591	30.9090	30.9007	**31.3353**
	0.7851	0.7745	0.8122	0.8518	0.8475	**0.8601**
Truck and APCs 7.1.06	29.1648	29.5127	30.2673	31.0977	31.0977	**31.5269**
	0.7880	0.7776	0.8157	0.8550	0.8508	**0.8629**

In Table 1, each cell 2 results shows: Top - image PSNR (dB), Bottom - SSIM index, which shows the improvement in PSNR and SSIM index by applying our method versus the other methods. The best result for each image are highlighted. It can be seen that the proposed CSHR outperforms all the other methods, including ScSR and TIP14 which stand for state-of-the-art method.

Also, we compare the running time of different state-of-the-art SR methods which is shown in Fig. 3:

In Fig. 3, x-axis means the size of image in pixel we use, y-axis is the average running time. It could be easily find that the running time of the baseline method

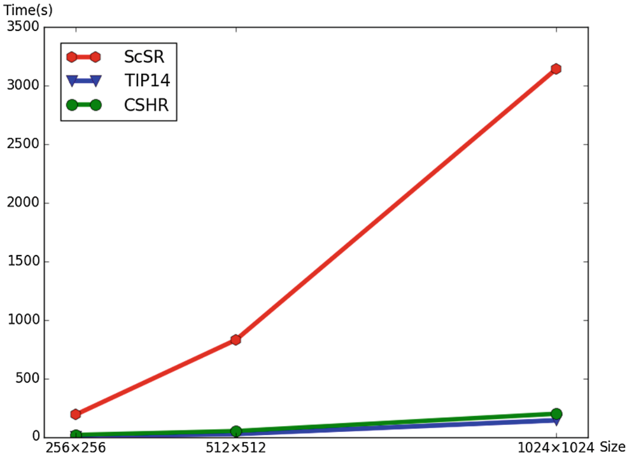

Fig. 3. Running time among the methods

ScSR is the longest. Obviously, TIP14 runs fastest, because it makes use of a statistical prediction model. Our proposed CSHR method works much faster than ScSR, while a little slower than TIP14. It means that the running time of CSHR is closing to the state-of-the-art method.

4 Conclusions

In this paper, in order to make use of the high speed and low quality SR results, we proposed a novel method CSHR for solving the SFSR problem. CSHR does not rely on any learning patches or over-complete dictionary, it is based on the consensus of other SR reconstructions. It makes a compressive sampling on these consensus hybrid in the pixel domain. By solving a convex optimization program, it recovers the HR image. We have also proved that with a high probability, the coherence between Φ and Ψ in CSHR is less than $\sqrt{2 \log N}$. Thus CS theory will ensure the efficiency of CSHR. Experimental results demonstrate the effectiveness of the CSHR. CSHR is able to achieve the state-of-the-art SR results. Our future work will focus on the choice of Ψ, perhaps wavelet basis is a good choice. We know the fact that wavelets automatically adapt to singularities in the image; important wavelet coefficients tend to cluster around edge contours, while large smooth regions can be built up with relatively few terms.

Acknowledgements. The authors wish to thank the authors of [9,14] for generously sharing their code and data with them.

This research is supported in part by the Major State Basic Research Development Program of China (973 Program, 2012CB315803), the National Natural Science Foundation of China (61371078), and the Research Fund for the Doctoral Program of Higher Education of China (20130002110051).

References

1. Candes, E., Romberg, J.: Sparsity and incoherence in compressive sampling. Inverse Prob. **23**(3), 969 (2007)
2. Candès, E.J., Romberg, J., Tao, T.: Robust uncertainty principles: exact signal reconstruction from highly incomplete frequency information. IEEE Trans. Inf. Theory **52**(2), 489–509 (2006)
3. Candes, E.J., Romberg, J.K., Tao, T.: Stable signal recovery from incomplete and inaccurate measurements. Commun. Pure Appl. Math. **59**(8), 1207–1223 (2006)
4. Candes, E.J., Tao, T.: Near-optimal signal recovery from random projections: universal encoding strategies? IEEE Trans. Inf. Theory **52**(12), 5406–5425 (2006)
5. Donoho, D.L.: Compressed sensing. IEEE Trans. Inf. Theory **52**(4), 1289–1306 (2006)
6. Donoho, D.L., Huo, X.: Uncertainty principles and ideal atomic decomposition. IEEE Trans. Inf. Theory **47**(7), 2845–2862 (2001)
7. Huynh-Thu, Q., Ghanbari, M.: Scope of validity of PSNR in image/video quality assessment. Electron. Lett. **44**(13), 800–801 (2008)
8. Park, S.C., Park, M.K., Kang, M.G.: Super-resolution image reconstruction: a technical overview. IEEE Signal Process. Mag. **20**(3), 21–36 (2003)
9. Peleg, T., Elad, M.: A statistical prediction model based on sparse representations for single image super-resolution. IEEE Trans. Image Process. publ. IEEE Signal Process. Soc. **23**(6), 2569–2582 (2014)
10. Romberg, J.: Imaging via compressive sampling [introduction to compressive sampling and recovery via convex programming]. IEEE Signal Process. Mag. **25**(2), 14–20 (2008)
11. Van Ouwerkerk, J.: Image super-resolution survey. Image Vis. Comput. **24**(10), 1039–1052 (2006)
12. Wang, Z., Bovik, A.C., Sheikh, H.R., Simoncelli, E.P.: Image quality assessment: from error visibility to structural similarity. IEEE Trans. Image Process. **13**(4), 600–612 (2004)
13. Yang, J., Wright, J., Huang, T., Ma, Y.: Image super-resolution as sparse representation of raw image patches. In: IEEE Conference on Computer Vision and Pattern Recognition, CVPR 2008, pp. 1–8. IEEE (2008)
14. Yang, J., Wright, J., Huang, T.S., Ma, Y.: Image super-resolution via sparse representation. IEEE Trans. Image Process. **19**(11), 2861–2873 (2010)
15. Zeyde, R., Elad, M., Protter, M.: On single image scale-up using sparse-representations. In: Boissonnat, J.-D., Chenin, P., Cohen, A., Gout, C., Lyche, T., Mazure, M.-L., Schumaker, L. (eds.) Curves and Surfaces 2011. LNCS, vol. 6920, pp. 711–730. Springer, Heidelberg (2012)